International Journal of Multimedia and Ubiquitous Engineering
Vol. 1, No. 3, September, 2006

TD-CDMA Systems Using Turbo Code for Mobile Multimedia Services

Seong Chul Cho, and Jin Up Kim
ETRI, Mobile Telecommunication Research Division,
161 Gajeong-dong Yuseong-gu, Daejeon, 305-350, Korea
{sccho, jukim}@etri.re.kr
http://www.etri.re.kr

Abstract In this paper, the performance of a wireless communication system based on the TD-CDMA transmission technique is analyzed. In this paper, we present simulation results for the performance of a turbo coded TD-CDMA system with QPSK over Rayleigh fading channel model. And the system performance employing the simple averaging channel estimation is compared to the ideal case with the perfect channel estimation.

Keyword: TD-CDMA, Turbo Code, Mobile Multimedia Services

1. Introduction

IMT-2000 system can provide the voice and data services as well as mobile multimedia service up to 2Mbps with low cost. It is expected to create enormous mobile market. In addition to aforementioned services, it is very important to provide mobile Internet with low cost to mobile subscriber.
By having introduced high-speed Internet service in wireline network, Korea has made enormous progress in the IT field. However, we have not done any research work to deliver this Internet service by wireless to end-users. The Internet service shows us the asymmetric traffic pattern between uplink and downlink compared to conventional voice and video service. UTRA TDD mode is very well suited to this mobile Internet service among the IMT-2000 technologies because of the flexible assignment of time slots to either downlink or uplink [1][2]. This TDD mode has almost similar protocol structure as WCDMA mode, but shows the different modem schemes to W-CDMA. If we get this difference, we will easily develop UTRA TDD system when it is commercialized.
The third generation mobile radio system UTRA that has been specified in the 3GPP consists of two modes, FDD mode and TDD mode. The agreement recommends the use of WCDMA for UTRA FDD and TD-CDMA for UTRA TDD. TD-CDMA is based on a combination of TDMA and CDMA, whereas W-CDMA is a pure CDMA-based system [1]. We have focused our energy to develop WCDMA and cdma2000 systems. Siemens has been developed this TD-CDMA technology for a few years but we did not developed it until now. In this paper, we have evaluated the performance of the TD-CDMA for mobile Internet services
The organization of this paper is as following. Section 2 introduces the characteristics of TDD systems, and analyzes the received signal to build the receiver structure. In section 3, we analyze the performance of the TD-CDMA systems. Finally, our investigations are summarized and concluded in section 4.

2. TD-CDMA System

The TD-CDMA system comprises standard TDMA slotted structures where in each time slot spreading techniques are used to allow simultaneous transmission by several users. The time slots are used in the sense of a TDMA component to separate different user signals in the time domain. The TDMA frame has a duration of 10 ms and is subdivided into 15 time slots of 2560*T_c duration each. A time slot corresponds to 2560 chips. The physical channel signal format is presented in fig.1 [3].

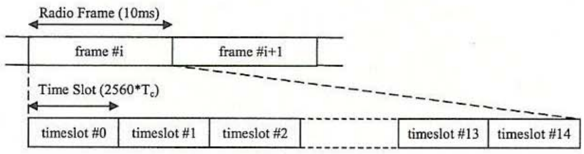

Fig. 1. Physical Channel Signal Format

Each 10 ms frame consists of 15 time slots, each allocated to either the uplink or the downlink. With such flexibility, the TDD mode can be adapted to different environments and deployment scenarios. In any configuration at least one time slot has to be allocated for the downlink and at least one time slot has to be allocated for the uplink.
A physical channel in TDD is a burst, which is transmitted in a particular timeslot within allocated radio frames. The allocation can be continuous, i.e. the time slot in every frame is allocated to the physical channel or discontinuous, i.e. the time slot in a subset of all frames is allocated only. Three types of bursts for dedicated physical channels are defined. All of them consist of two data symbol fields, a midamble and a guard period, the lengths of which are different for the individual burst types. The burst type 1 is shown in fig. 2.

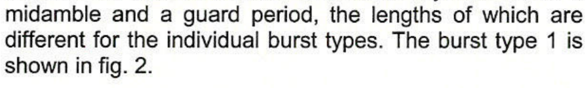

Fig. 2. Burst Structure of the Burst Type I

The duration of a burst is one time slot. Several bursts can be transmitted at the same time from one transmitter. In this case, the data parts must use different OVSF channelisation codes, but the same scrambling code. The midamble parts are either identically or differently shifted versions of a cell-specific basic midamble code [3].
The data part of the burst is spread with a combination of

channelisation code and scrambling code. The channelisation code is a OVSF code, which can have a spreading factor of 1, 2, 4, 8, or 16. The data rate of the physical channel is depending on the used spreading factor of the used OVSF code. Downlink physical channels shall use spreading factor of 16. Multiple parallel physical channels can be used to support higher data rates. These parallel physical channels shall be transmitted using different channelisation codes. Operation with a single code with spreading factor 1 is possible for the downlink physical channels. The range of spreading factor that may be used for uplink physical channels shall range from 16 down to 1 [3].

The data modulation is performed to the bits from the output of the physical channel mapping procedure and combines always 2 consecutive binary bits to a complex valued data symbol. Each user burst has two data carrying parts, termed data blocks:

$$\underline{\mathbf{d}}^{(k,i)} = \left(\underline{d}_1^{(k,i)}, \underline{d}_2^{(k,i)}, \ldots, \underline{d}_{N_k}^{(k,i)}\right)^T, \quad i = 1,2; k = 1,\ldots,K_{Code} \qquad (1)$$

K_{Code} is the number of used codes in a time slot, max K_{Code} =16. N_k is the number of symbols per data field for the code k. This number is linked to the spreading factor q_k [3]. Data block $\underline{\mathbf{d}}^{(k,1)}$ is transmitted before the midamble and data block $\underline{\mathbf{d}}^{(k,2)}$ after the midamble. The complex-valued chip sequence is QPSK modulated as shown in fig. 3.

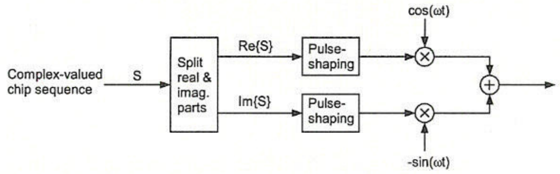

Fig. 3. Modulation of Complex Valued Chip Sequences

The data modulation is QPSK, thus the data symbols $\underline{d}_n^{(k,i)}$ are generated from two consecutive data bits from the output of the physical channel mapping procedure:

$$b_{l,n}^{(k,i)} \in \{0,1\}, \quad l = 1,2; k = 1,\ldots,K_{Code}; n = 1,\ldots,N_k; i = 1,2 \qquad (2)$$

using the following mapping to complex symbols:

Table 1. Symbol Mapping in TDD

consecutive binary bit pattern	complex symbol
$b_{1,n}^{(k,i)}\ b_{2,n}^{(k,i)}$	$\underline{d}_n^{(k,i)}$
00	+j
01	+1
10	-1
11	-j

In the following fig. 4 shows the transmitter structure of the TDD system. In this Figure, the coded signals are mapped to the complex symbols for spreading and channelizing. The mapped symbols are spreaded by the orthogonal channel code which is the real value having the maximum length of 16. Then, the mapped symbols are scrambled by the encrypted code. This encrypted code is unique in each cell and it has the length of 16.

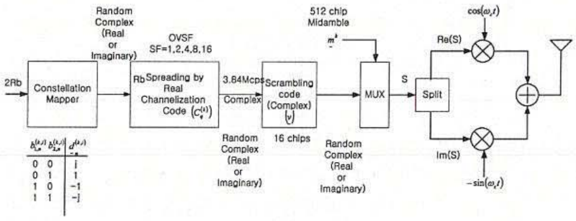

Fig. 4. Structure of Transmitter in TDD System

The following Eq. (3) shows the transmitted signal *s(t)* from the transmitter in fig.4. The signal is composed of $s_{II}(t)$, $s_{QQ}(t)$, $s_{IQ}(t)$, and $s_{QI}(t)$.

$$\begin{aligned}
s_{II}(t) &= \sqrt{E_c}\, d_{I,n}^k\, C_q^k\, V_I^k \cos(\omega_c t) \\
s_{QQ}(t) &= -\sqrt{E_c}\, d_{Q,n}^k\, C_q^k\, V_Q^k \cos(\omega_c t) \\
s_{IQ}(t) &= -\sqrt{E_c}\, d_{I,n}^k\, C_q^k\, V_Q^k \sin(\omega_c t) \\
s_{QI}(t) &= -\sqrt{E_c}\, d_{Q,n}^k\, C_q^k\, V_I^k \sin(\omega_c t)
\end{aligned} \qquad (3)$$

It is assumed that a data modulator has the pulse shaping filter for a same phase signal and orthogonal phase signal. Then, based on the Eq. (3), the mobile station's transmitted signal *s(t)* can be expressed as $s_{II}(t)$, $s_{QQ}(t)$, $s_{IQ}(t)$, and $s_{QI}(t)$.

$$\begin{aligned}
s_{II}(t) &= \sum_{n=1}^{q} \sqrt{E_c}\, d_{I,n}^k\, C_n^k\, V_{I,n}^k\, h(t - nT_c)\cos(\omega_c t) \\
s_{QQ}(t) &= -\sum_{n=1}^{q} \sqrt{E_c}\, d_{Q,n}^k\, C_n^k\, V_{Q,n}^k\, h(t - nT_c)\cos(\omega_c t) \\
s_{IQ}(t) &= -\sum_{n=1}^{q} \sqrt{E_c}\, d_{I,n}^k\, C_n^k\, V_{Q,n}^k\, h(t - nT_c)\sin(\omega_c t) \\
s_{QI}(t) &= -\sum_{n=1}^{q} \sqrt{E_c}\, d_{Q,n}^k\, C_n^k\, V_{I,n}^k\, h(t - nT_c)\sin(\omega_c t)
\end{aligned} \qquad (4)$$

And, after undergoing the frequency selective fading channel, the base station received signal *r(t)* is expressed as $r_{II}(t)$, $r_{QQ}(t)$, $r_{IQ}(t)$, and $r_{QI}(t)$.

$$\begin{aligned}
r_{II}(t) &= \sum_{j=1}^{N_p} \alpha_j \sum_{n=1}^{q} \sqrt{E_c}\, d_{I,n}^k\, C_n^k\, V_{I,n}^k\, h(t - nT_c - \tau_j)\cos(\omega_c t - \theta_j) + n_I(t)\cos(\omega_c t) \\
r_{QQ}(t) &= -\sum_{j=1}^{N_p} \alpha_j \sum_{n=1}^{q} \sqrt{E_c}\, d_{Q,n}^k\, C_n^k\, V_{Q,n}^k\, h(t - nT_c - \tau_j)\cos(\omega_c t - \theta_j) + n_I(t)\cos(\omega_c t) \\
r_{IQ}(t) &= -\sum_{j=1}^{N_p} \alpha_j \sum_{n=1}^{q} \sqrt{E_c}\, d_{I,n}^k\, C_n^k\, V_{Q,n}^k\, h(t - nT_c - \tau_j)\sin(\omega_c t - \theta_j) - n_Q(t)\sin(\omega_c t) \\
r_{QI}(t) &= -\sum_{j=1}^{N_p} \alpha_j \sum_{n=1}^{q} \sqrt{E_c}\, d_{Q,n}^k\, C_n^k\, V_{I,n}^k\, h(t - nT_c - \tau_j)\sin(\omega_c t - \theta_j) - n_Q(t)\sin(\omega_c t)
\end{aligned} \qquad (5)$$

For the analysis, the receiver structure is assumed to the orthogonal demodulation structure. And the same phase components and the orthogonal phase components are analyzed, and the results are summarized.

When the mobile station transmits two kinds of the same phase signal $r_{II}(t)$ and $r_{QQ}(t)$, the analysis of the base station received signal is as following. First of all, after passing the LPF, Sampler, and matched filter, the same phase signal can be expressed as Eq. (6), (7), (8) and (9).

$$\begin{aligned}
r_{II}(t) \times \cos(\omega_c t) &= \sum_{j=1}^{N_p} \alpha_j \sum_{n=1}^{q} \sqrt{E_c}\, d_{I,n}^k\, C_n^k\, V_{I,n}^k\, h(t - nT_c - \tau_j)\cos(\omega_c t - \theta_j) \times \cos(\omega_c t) \\
&\quad + n_I(t)\cos(\omega_c t) \times \cos(\omega_c t) \\
&= \sum_{j=1}^{N_p} \alpha_j \sum_{n=1}^{q} \sqrt{E_c}\, d_{I,n}^k\, C_n^k\, V_{I,n}^k\, h(t - nT_c - \tau_j)\frac{\cos(\theta_j) + \cos(2\omega_c t - \theta_j)}{2} \\
&\quad + n_I(t)\frac{1 + \cos(2\omega_c t)}{2}
\end{aligned} \qquad (6)$$

$$r_{QQ}(t)\times\cos(\omega_c t)=-\sum_{j=1}^{N_p}\alpha_j\sum_{n=1}^{q}\sqrt{E_c}\ d_{Q,n}^k\,C_n^k\,V_{Q,n}^k\,h(t-nT_c-\tau_j)\cos(\omega_c t-\theta_j)\times\cos(\omega_c t)$$
$$+n_I(t)\cos(\omega_c t)\times\cos(\omega_c t)$$
$$=-\sum_{j=1}^{N_p}\alpha_j\sum_{n=1}^{q}\sqrt{E_c}\ d_{Q,n}^k\,C_n^k\,V_{Q,n}^k\,h(t-nT_c-\tau_j)\frac{\cos(\theta_j)+\cos(2\omega_c t-\theta_j)}{2}$$
$$+n_I(t)\frac{1+\cos(2\omega_c t)}{2} \quad (7)$$

$$r_{II}(t)\times\cos(\omega_c t)\Big|_{LPF}=\sum_{j=1}^{N_p}\alpha_j\sum_{n=1}^{q}\sqrt{E_c}\ d_{I,n}^k\,C_n^k\,V_{I,n}^k\,R(mT_c-nT_c-\tau_j)\frac{\cos(\theta_j)}{2}+\frac{n_I^{\bullet}(mT_c)}{2} \quad (8)$$

$$r_{QQ}(t)\times\cos(\omega_c t)\Big|_{LPF}=-\sum_{j=1}^{N_p}\alpha_j\sum_{n=1}^{q}\sqrt{E_c}\ d_{Q,n}^k\,C_n^k\,V_{Q,n}^k\,R(mT_c-nT_c-\tau_j)\frac{\cos(\theta_j)}{2}+\frac{n_I^{\bullet}(mT_c)}{2} \quad (9)$$

Also the orthogonal phase component signals can be expressed as Eq. (10), (11), (12), and (13).

$$r_{II}(t)\times\sin(\omega_c t)=\sum_{j=1}^{N_p}\alpha_j\sum_{n=1}^{q}\sqrt{E_c}\ d_{I,n}^k\,C_n^k\,V_{I,n}^k\,h(t-nT_c-\tau_j)\cos(\omega_c t-\theta_j)\times\sin(\omega_c t)$$
$$+n_I(t)\cos(\omega_c t)\times\sin(\omega_c t)$$
$$=\sum_{j=1}^{N_p}\alpha_j\sum_{n=1}^{q}\sqrt{E_c}\ d_{I,n}^k\,C_n^k\,V_{I,n}^k\,h(t-nT_c-\tau_j)\frac{-\sin(-\theta_j)+\sin(2\omega_c t-\theta_j)}{2}$$
$$+n_I(t)\frac{\sin(0)+\sin(2\omega_c t)}{2} \quad (10)$$

$$r_{QQ}(t)\times\sin(\omega_c t)=-\sum_{j=1}^{N_p}\alpha_j\sum_{n=1}^{q}\sqrt{E_c}\ d_{Q,n}^k\,C_n^k\,V_{Q,n}^k\,h(t-nT_c-\tau_j)\cos(\omega_c t-\theta_j)\times\sin(\omega_c t)$$
$$+n_I(t)\cos(\omega_c t)\times\sin(\omega_c t)$$
$$=-\sum_{j=1}^{N_p}\alpha_j\sum_{n=1}^{q}\sqrt{E_c}\ d_{Q,n}^k\,C_n^k\,V_{Q,n}^k\,h(t-nT_c-\tau_j)\frac{-\sin(-\theta_j)+\sin(2\omega_c t-\theta_j)}{2}$$
$$+n_I(t)\frac{\sin(0)+\sin(2\omega_c t)}{2} \quad (11)$$

$$r_{II}(t)\times\sin(\omega_c t)\Big|_{LPF}=\sum_{j=1}^{N_p}\alpha_j\sum_{n=1}^{q}\sqrt{E_c}\ d_{I,n}^k\,C_n^k\,V_{I,n}^k\,R(mT_c-nT_c-\tau_j)\frac{\sin(\theta_j)}{2} \quad (12)$$

$$r_{QQ}(t)\times\sin(\omega_c t)\Big|_{LPF}=-\sum_{j=1}^{N_p}\alpha_j\sum_{n=1}^{q}\sqrt{E_c}\ d_{Q,n}^k\,C_n^k\,V_{Q,n}^k\,R(mT_c-nT_c-\tau_j)\frac{\sin(\theta_j)}{2} \quad (13)$$

The demodulated data is obtained by multiplying same phase and orthogonal phase signal expressed Eq. (8), (9), (12), and (13) by same phase/orthogonal phase code, respectively. As the result, the demodulator structure of the base station can be the fig. 5.

When the mobile station transmits two kinds of orthogonal phase signal $r_{IQ}(t)$ and $r_{QI}(t)$, the analysis of the base station received signals is as following. Then, after passing the LPF, Sampler, and matched filter, the orthogonal phase signal can be expressed as Eq. (14), (15), (16) and (17).

$$r_{IQ}(t)\times\cos(\omega_c t)=-\sum_{j=1}^{N_p}\alpha_j\sum_{n=1}^{q}\sqrt{E_c}\ d_{I,n}^k\,C_n^k\,V_{Q,n}^k\,h(t-nT_c-\tau_j)\sin(\omega_c t-\theta_j)\times\cos(\omega_c t)$$
$$-n_Q(t)\sin(\omega_c t)\times\cos(\omega_c t)$$
$$=-\sum_{j=1}^{N_p}\alpha_j\sum_{n=1}^{q}\sqrt{E_c}\ d_{I,n}^k\,C_n^k\,V_{Q,n}^k\,h(t-nT_c-\tau_j)\frac{\sin(-\theta_j)+\sin s(2\omega_c t-\theta_j)}{2}$$
$$-n_Q(t)\frac{\sin(0)+\sin(2\omega_c t)}{2} \quad (14)$$

$$r_{QI}(t)\times\cos(\omega_c t)=-\sum_{j=1}^{N_p}\alpha_j\sum_{n=1}^{q}\sqrt{E_c}\ d_{Q,n}^k\,C_n^k\,V_{I,n}^k\,h(t-nT_c-\tau_j)\sin(\omega_c t-\theta_j)\times\cos(\omega_c t)$$
$$-n_Q(t)\sin(\omega_c t)\times\cos(\omega_c t)$$
$$=-\sum_{j=1}^{N_p}\alpha_j\sum_{n=1}^{q}\sqrt{E_c}\ d_{Q,n}^k\,C_n^k\,V_{Q,n}^k\,h(t-nT_c-\tau_j)\frac{\sin(-\theta_j)+\sin(2\omega_c t-\theta_j)}{2}$$
$$-n_Q(t)\frac{\sin(0)+\sin(2\omega_c t)}{2} \quad (15)$$

$$r_{IQ}(t)\times\cos(\omega_c t)\Big|_{LPF}=\sum_{j=1}^{N_p}\alpha_j\sum_{n=1}^{q}\sqrt{E_c}\ d_{I,n}^k\,C_n^k\,V_{Q,n}^k\,R(mT_c-nT_c-\tau_j)\frac{\sin(\theta_j)}{2} \quad (16)$$

$$r_{QI}(t)\times\cos(\omega_c t)\Big|_{LPF}=\sum_{j=1}^{N_p}\alpha_j\sum_{n=1}^{q}\sqrt{E_c}\ d_{Q,n}^k\,C_n^k\,V_{I,n}^k\,R(mT_c-nT_c-\tau_j)\frac{\sin(\theta_j)}{2} \quad (17)$$

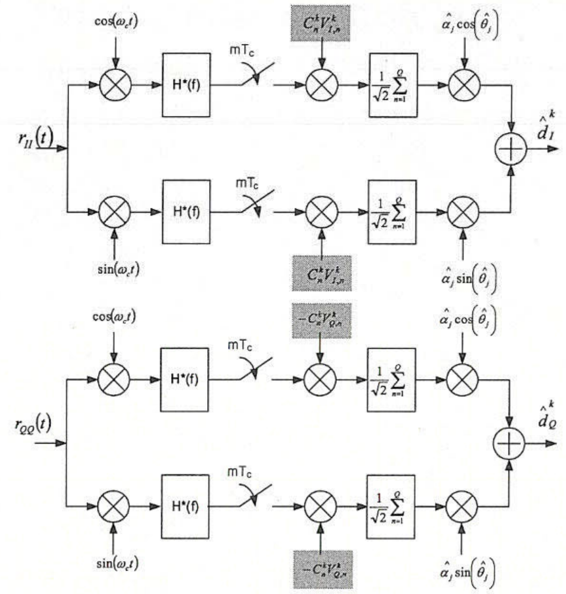

Fig.5. Demodulator Structure for Same Phase Components

When the mobile station transmits two kinds of orthogonal phase signal $r_{IQ}(t)$ and $r_{QI}(t)$, the analysis of the base station received signals is as following. Then, after passing the LPF, Sampler, and matched filter, the orthogonal phase signal can be expressed as Eq. (14), (15), (16) and (17).

$$r_{IQ}(t)\times\cos(\omega_c t)=-\sum_{j=1}^{N_p}\alpha_j\sum_{n=1}^{q}\sqrt{E_c}\ d_{I,n}^k\,C_n^k\,V_{Q,n}^k\,h(t-nT_c-\tau_j)\sin(\omega_c t-\theta_j)\times\cos(\omega_c t)$$
$$-n_Q(t)\sin(\omega_c t)\times\cos(\omega_c t)$$
$$=-\sum_{j=1}^{N_p}\alpha_j\sum_{n=1}^{q}\sqrt{E_c}\ d_{I,n}^k\,C_n^k\,V_{Q,n}^k\,h(t-nT_c-\tau_j)\frac{\sin(-\theta_j)+\sin s(2\omega_c t-\theta_j)}{2}$$
$$-n_Q(t)\frac{\sin(0)+\sin(2\omega_c t)}{2} \quad (18)$$

$$r_{QI}(t)\times\cos(\omega_c t)=-\sum_{j=1}^{N_p}\alpha_j\sum_{n=1}^{q}\sqrt{E_c}\ d_{Q,n}^k\,C_n^k\,V_{I,n}^k\,h(t-nT_c-\tau_j)\sin(\omega_c t-\theta_j)\times\cos(\omega_c t)$$
$$-n_Q(t)\sin(\omega_c t)\times\cos(\omega_c t)$$
$$=-\sum_{j=1}^{N_p}\alpha_j\sum_{n=1}^{q}\sqrt{E_c}\ d_{Q,n}^k\,C_n^k\,V_{Q,n}^k\,h(t-nT_c-\tau_j)\frac{\sin(-\theta_j)+\sin(2\omega_c t-\theta_j)}{2}$$
$$-n_Q(t)\frac{\sin(0)+\sin(2\omega_c t)}{2} \quad (19)$$

$$r_{IQ}(t)\times\cos(\omega_c t)\Big|_{LPF}=\sum_{j=1}^{N_p}\alpha_j\sum_{n=1}^{q}\sqrt{E_c}\ d_{I,n}^k\,C_n^k\,V_{Q,n}^k\,R(mT_c-nT_c-\tau_j)\frac{\sin(\theta_j)}{2} \quad (20)$$

$$r_{QI}(t)\times\cos(\omega_c t)\Big|_{LPF}=\sum_{j=1}^{N_p}\alpha_j\sum_{n=1}^{q}\sqrt{E_c}\ d_{Q,n}^k\,C_n^k\,V_{I,n}^k\,R(mT_c-nT_c-\tau_j)\frac{\sin(\theta_j)}{2} \quad (21)$$

Also the orthogonal phase component signals can be expressed as Eq. (18), (19), (20), and (21).

$$r_{IQ}(t)\times\sin(\omega_c t)=-\sum_{j=1}^{N_p}\alpha_j\sum_{n=1}^{q}\sqrt{E_c}\ d_{I,n}^k\,C_n^k\,V_{Q,n}^k\,h(t-nT_c-\tau_j)\sin(\omega_c t-\theta_j)\times\sin(\omega_c t)$$
$$-n_Q(t)\sin(\omega_c t)\times\sin(\omega_c t)$$
$$=-\sum_{j=1}^{N_p}\alpha_j\sum_{n=1}^{q}\sqrt{E_c}\ d_{I,n}^k\,C_n^k\,V_{Q,n}^k\,h(t-nT_c-\tau_j)\frac{\cos(\theta_j)-\cos(2\omega_c t-\theta_j)}{2}$$
$$-n_Q(t)\frac{1-\cos(2\omega_c t)}{2} \quad (22)$$

$$r_{QI}(t)\times\sin(\omega_c t) = -\sum_{j=1}^{N_p}\alpha_j\sum_{n=1}^{q}\sqrt{E_c}\; d_{Q,n}^k\, C_n^k\, V_{I,n}^k\, h(t-nT_c-\tau_j)\sin(\omega_c t-\theta_j)\times\sin(\omega_c t) - n_Q(t)\sin(\omega_c t)\times\sin(\omega_c t)$$
$$= -\sum_{j=1}^{N_p}\alpha_j\sum_{n=1}^{q}\sqrt{E_c}\; d_{Q,n}^k\, C_n^k\, V_{I,n}^k\, h(t-nT_c-\tau_j)\frac{\cos(\theta_j)-\cos(2\omega_c t-\theta_j)}{2} - n_Q(t)\frac{1-\cos(2\omega_c t)}{2} \quad (23)$$

$$r_{IQ}(t)\times\sin(\omega_c t)\big|_{LPF} = -\sum_{j=1}^{N_p}\alpha_j\sum_{n=1}^{q}\sqrt{E_c}\; d_{I,n}^k\, C_n^k\, V_{Q,n}^k\, R(mT_c-nT_c-\tau_j)\frac{\cos(\theta_j)}{2} - \frac{n_Q^*(mT_c)}{2} \quad (24)$$

$$r_{QI}(t)\times\sin(\omega_c t)\big|_{LPF} = -\sum_{j=1}^{N_p}\alpha_j\sum_{n=1}^{q}\sqrt{E_c}\; d_{Q,n}^k\, C_n^k\, V_{I,n}^k\, R(mT_c-nT_c-\tau_j)\frac{\cos(\theta_j)}{2} + \frac{n_Q^*(mT_c)}{2} \quad (25)$$

The demodulated data is obtained by multiplying same phase and orthogonal phase signal expressed Eq. (16), (17), (20), and (21) by same phase/orthogonal phase code. As the result, the demodulator structure of base station can be the fig. 6.

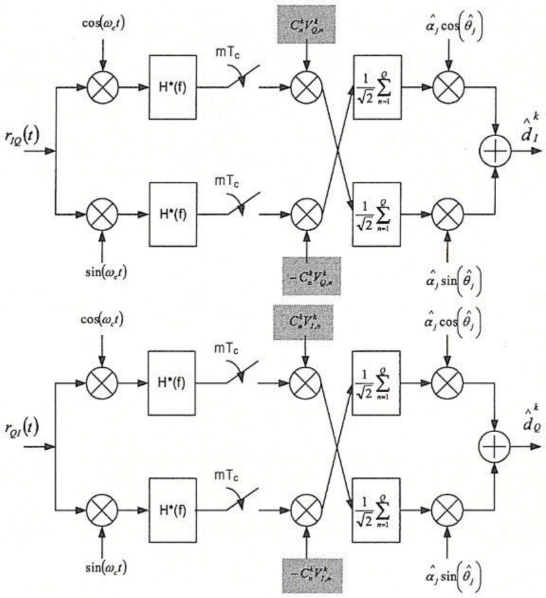

Fig. 6. Demodulator Structure for Orthogonal Phase Components

From such analysis, same phase and orthogonal phase signals transmitted by a mobile station are expressed Eq. (8), (9), (12), and (13) and Eq. (16), (17), (20), and (21). Base on these equations, the structure of base station's demodulator is shown in fig. 7.

3. Simulations

For the simulation, this paper assumes some cases.
At first, 3.84Mcps TDD system is considered.
And secondly, it is assumed that there is no guard interval in burst type 1.
At third, the data frame is consisted of one timeslot unit having 2560 chips.
Finally, it is assumed that the power control and frame synchronization is perfect.
Table 2 shows the parameters of the simulations.

Table 2. Parameters for Simulation

Parameters	Value
Chip rate	3.84 Mcps
Channel code	Turbo code 1/2 [4]
Decoding algorithm	MAP
Number of iteration	8
Burst type	Type I
Spreading factor	16
Channel model	Rayleigh fading (1, and 3 path) Jakes' power spectrum [5]
Mobile Speed	10km/h, 60km/h
Channel estimator	Ideal / non-ideal (SA algorithm)

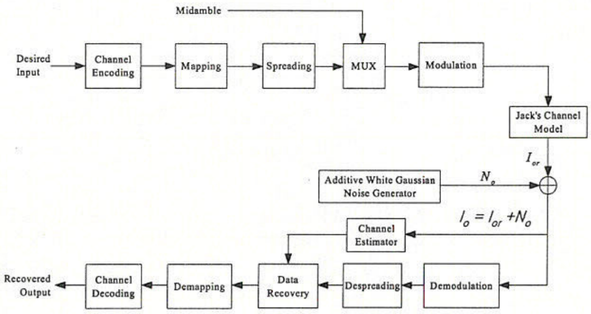

Fig. 8. Structure of the Simulator

In this simulation, the internal interleaver size of turbo code is 128 bits, and 8 times iteration is used. Also for the multipath simulation, 0.5, 0.3 and 0.2 are selected for the weight factors in 3-path. fig. 9 and fig 10 show the performance of TD-CDMA system using turbo code.

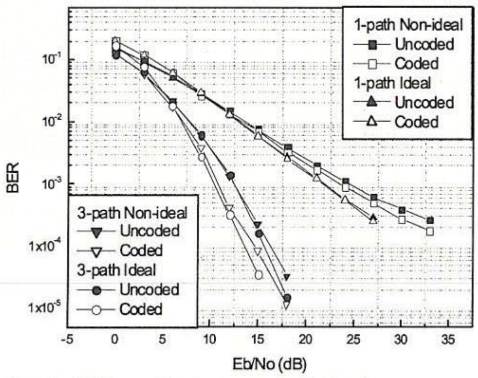

Fig. 9. BER performance at v=10km/h

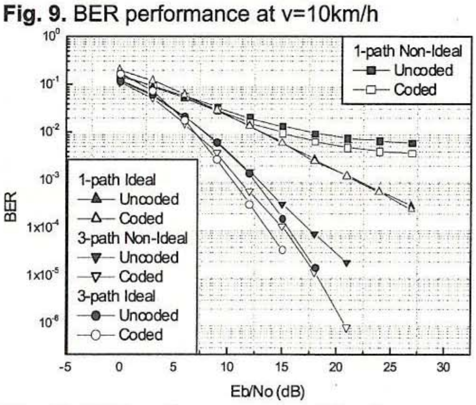

Fig. 10. BER performance at v=60km/h

4. Conclusion

In this paper, we propose and analyze a channel estimator and data demodulator structures for the TD-CDMA system, which is a TDD-based CDMA system, one of third-generation mobile communication systems. We analyze the performance of the TD-CDMA system using turbo code over mobile channel environments.

As the results of the simulations, it is shown that turbo code has better coding gains in case the fast moving channel when lower BER is required. Also, the simulation results confirm the good performance of the RAKE receiver in the multipath environment. For 10km/h mobile speed, SA channel estimation method shows the performance near to the ideal channel estimation.

However for the high mobile speed, it shows the performance different from the ideal channel estimation. In order to improve the performance over high speed mobile channel, more efficient channel estimation algorithm is required.

References

[1] M. Haardt, A. Klein, R. Koehn, S. Oestreich, M. Purat, V. Sommer, and T. Ulrich, "The TD-CDMA based UTRA TDD mode," IEEE Journal on Selected Areas in Communications, vol. 18, no. 8, pp. 1375-1385, Aug. 2000.

[2] M. Haardt, A. Klein, S. Oestreich, M.purat, V. Sommer and T. Ulrich, "The physical layer of UTRA TDD", in Proc. IEEE Vehicular Technology Conference (VTC'00 Spring), vol. 2, pp. 1175-1180, May 2000.

[3] 3GPP TS 25.221, Physical channels and mapping of transport channels onto physical channels (TDD), The 3rd Generation Partnership Project, ver. 4.0.0 Mar. 2001.

[4] 3GPP TS 25.222, Multiplexing and channel coding (TDD), The 3rd Generation Partnership Project, ver. 4.0.0 Mar. 2001.

[5] W. C. Jakes, Micorwave mobile communications, Wiley-IEEE Press, May 1994.